Photovoltaic Fault Detection Algorithm Based on Theoretical Curves Modelling and Fuzzy Classification System

Mahmoud Dhimish, Violeta Holmes, Bruce Mehrdadi, Mark Dales, Peter Mather

Department of Computing and Engineering, University of Huddersfield, Huddersfield, United Kingdom

Abstract

This work proposes a fault detection algorithm based on the analysis of the theoretical curves which describe the behaviour of an existing grid-connected photovoltaic (GCPV) plant. For a given set of working conditions, solar irradiance and PV modules' temperature, a number of attributes such as voltage ratio (VR) and power ratio (PR) are simulated using virtual instrumentation (VI) LabVIEW software. Furthermore, a third order polynomial function is used to generate two detection limits (high and low limit) for the VR and PR ratios obtained using LabVIEW simulation tool.

The high and low detection limits are compared with real-time long-term data measurements from a 1.1kWp GCPV system installed at the University of Huddersfield, United Kingdom. Furthermore, samples that lies out of the detection limits are processed by a fuzzy logic classification system which consists of two inputs (VR and PR) and one output membership function.

The obtained results show that the fault detection algorithm can accurately detect different faults occurring in the PV system. The maximum detection accuracy of the algorithm before considering the fuzzy logic system is equal to 95.27%, however, the fault detection accuracy is increased up to a minimum value of 98.8% after considering the fuzzy logic system.

Keywords: Photovoltaic Faults, Fault Detection, Fuzzy Logic, PV Hot Spot Detection, LabVIEW.

1. INTRODUCTION

Despite the fact that Grid-Connected Photo-Voltaic (GCPV) systems have no moving parts, and therefore usually require low maintenance, they are still subject to various failures and faults associated with the PV arrays, batteries, power conditioning units, utility interconnections and wiring [1 and 2]. It is especially difficult to shut down PV modules completely during faulty conditions related to PV arrays (DC side) [3]. It is therefore required to create algorithms to facilitate the detection of possible faults occurring in GCPV systems [4].

There are existing fault detection techniques for use in GCPV plants. Some use satellite data for fault prediction as presented by M. Tadj et al [5], this approach is based on satellite image for estimating solar radiation data and predicting faults occurring in the DC side of the GCPV plant. However, some algorithms do not require any climate data, such as solar irradiance and modules' temperature, but instead use earth capacitance measurements in a technique established by Taka-Shima el al [6].

Some fault detection methods use an automatic supervision based on the analysis of the output power for the GCPV system. A. Chouder & S. Silvestre et al [7], presented a new automatic supervision and fault detection technique which use a standard deviation method ($\pm 2\sigma$) for detecting various faults in PV systems such as faulty modules in a PV string and faulty maximum power point tracking (MPPT) units. However, S. Silverstre at al [8] presented a new fault detection algorithm based on the evaluation of the current and output voltage indicators for analyzing the type of fault occurred in PV systems installations.

A photovoltaic fault detection technique based on artificial neural network (ANN) is proposed by W. Chine et al [9]. The technique is based on the analysis of the voltage, power and the number of peaks in the current-voltage (I-V) curve characteristics. However, [10 and11], proposed a fault detection algorithm which allows the detection of seven different fault modes on the DC-side of the GCPV system. The algorithm uses the t-test statistical analysis technique for identifying the presence of systems fault conditions.

Other fault detection algorithms focus on faults occurring on the AC-side of GCPV systems, as proposed by R. Platon et al [12]. The approach uses $\pm 3\sigma$ statistical analysis technique for identifying the faulty conditions in the DC/AC inverter units. Moreover, hot-spot detection in PV substrings using the AC parameters characterization was developed by [13]. The hot-spot detection method can be further used and integrated with DC/DC power converters that operates at the subpanel level. Nevertheless, the hot spot mitigation due to the impact of micro cracks is described in [14].

A comprehensive review of the faults, trends and challenges of the grid-connected PV systems is explained by M. Obi & R.Bass, M. Alam et al and A. khamis et al [15-17].

Currently, fuzzy logic systems widely used with GCPV plants. R. Boukenoui et al [18] proposed a new intelligent MPPT method for standalone PV system operating under fast transient variations based on fuzzy logic controller (FLC) with scanning and storing algorithm. Furthermore, [19] presents an adaptive FLC design technique for PV inverters using differential search algorithm.

B. Abdesslam et al [20] proposed a neuro-fuzzy classifier for fault detection and classification in PV systems, the approach is suitable for detection faulty conditions such as detected bypass diodes and blocking diodes faults. Furthermore, [21] proposed a cascaded fuzzy logic based arc fault detection in PV modules using an analog-digital converter (ADC) contained in micro controllers.

Since many fault detection algorithms use statistical analysis techniques such as [7, 10, 11 and 12], this work proposes a fault detection algorithm that does not depend on any statistical approaches in order to classify faulty conditions in PV systems. Furthermore, some existing fault detection techniques such as [22 and 23] use a complex power circuit design to facilitate the fault detection in GCPV plants. However, the proposed fault detection algorithm depends only on the variations of the voltage and the power, which makes the algorithm simple to construct and reused in wide range of GCPV plants.

In this work, we present the development of a fault detection algorithm which allows the detection of possible faults occurring on the DC-side of GCPV systems. The algorithm is based on the analysis of theoretical voltage ratio (VR) and power ratio (PR) for the examined GCPV system. High and low detection limits are generated using 3^{rd} order polynomial functions which are obtained using the simulated data of the VR and PR ratios. Subsequently, if the theoretical curves are not capable to detect the type of the fault occurred in the GCPV system, a fuzzy logic classifier system is designed to facilitate the fault type detecting for the examined PV system. A software tool is designed using Virtual Instrumentation (VI) LabVIEW software to automatically display and monitor the possible faults occurring within the

GCPV plant. A LabVIEW VI is also used to log the measured power, voltage and current data for the entire GCPV system, more details regarding the VI LabVIEW structure is presented in [24].

The main contribution of this work is the theoretical implementation of a simple, fast and reliable GCPV fault detection algorithm. The algorithm does not depend on any statistical techniques which makes it easier to facilitate and detect faults based on theoretical curves analysis and fuzzy logic classification system. In practice, the proposed fault detection algorithm is capable of localizing and identifying faults occurring on the DC-side of GCPV systems. The types of fault which can be detected are based on the size of the GCPV plant, which will be discussed in the next section. The algorithm is based on a six layer method working sequentially as shown in Fig. 1.

This paper is organized as follows: Section 2 describes the methodology used which includes the PV theoretical power curve modelling and the proposed fault detection algorithm, while section 3 explains the validation and a brief discussion of the proposed fault detection algorithm. Finally, section 4 describes the conclusion and future work.

2. METHODOLOGY

2.1 Photovoltaic Theoretical Power Curve Modelling

The DC side of the GCPV system is modelled using the 5-parameter model. The voltage and current characteristics of the PV module can be obtained using the single diode model [25] as shown in (1).

$$\mathrm{I} = \mathrm{I_{ph}} - \mathrm{I_o}\left(\mathrm{e}^{\frac{\mathrm{V+IR_s}}{\mathrm{nsV_t}}} - 1\right) - \left(\frac{\mathrm{V+IR_s}}{\mathrm{R_{sh}}}\right) \quad (1)$$

Where I_{ph} is the photo-generated current at STC , I_o is the dark saturation current at STC, R_s is the module series resistance, R_{sh} is the panel parallel resistance, ns is the number of series cells in the PV module and V_t is the thermal voltage and it can be defined based on (2).

$$\mathrm{V_t} = \frac{\mathrm{A\,K\,T}}{\mathrm{q}} \quad (2)$$

Where A the ideal diode factor, k is Boltzmann's constant and q is the charge of the electron.

The five parameter model is determined by solving the transcendental equation (1) using Newton-Raphson algorithm [26] based only on the datasheet of the available parameters for the examined PV module that was used in this work as shown in Table 1. The power produced by the PV module in Watts can be easily calculated along with the current (I) and voltage (V) that is generated by equation (1), therefore:

$$\mathrm{P_{theoretical}} = \mathrm{I} \times \mathrm{V} \quad (3)$$

The Power-Voltage (P-V) curve analysis of the tested PV module is shown in Fig. 2. The maximum power and voltage for each irradiance level under the same temperature value can be expressed by the P-V curves.

The purpose of using the analysis for the P-V curves, is to generate the expected output power of the examined PV module, therefore, it can be used to predict the error between the measured PV data and the theoretical power and voltage performance.

The proposed PV fault detection algorithm can detect various fault in the GCPV plants such as:

- Partial shading (PS) condition effects the GCPV system
- 1 Faulty PV module and PS
- 2 Faulty PV modules and PS
- 3 Faulty PV modules and PS
    -
    -
    -
- (n-1) Faulty PV modules and PS, where n is the total number of PV modules in the GCPV installation.

In this paper, faulty PV module corresponds to a short-circuited PV module. Moreover, A briefly explanation of the proposed fault detection algorithm is presented in section 2.2 and section 2.3.

2.2 Proposed Fault Detection Algorithm: Theoretical Curves Modelling

The main objective of the fault detection algorithm is to detect and determine when and where a fault has occurred in the GCPV plant.

The first layer of the fault detection algorithm passes the measured irradiance level and photovoltaic module's temperature to VI LabVIEW software in order to generate the expected theoretical P-V curve as described previously in section 2.1. This layer is shown in Fig. 3.

To determine if a fault has occurred in a GCPV system, two ratios have been identified. The theoretical Power ratio (PR) and the theoretical voltage ratio (VR) have been used to categorize the region of the fault. It is necessary to use both ratios because:

1. Both ratios are changeable during faulty conditions in the PV systems
2. When the power ratio is equal to zero, the voltage ratio can still have a value regarding the voltage open circuit of the PV modules

The power and voltage ratios are given by the following expressions:

$$\mathrm{PR} = \frac{\mathrm{P_{G,T}}}{\mathrm{P_{G,T}} - \mathrm{nP_0}} \tag{4}$$

$$\mathrm{VR} = \frac{\mathrm{V_{G,T}}}{\mathrm{V_{G,T}} - \mathrm{nV_0}} \tag{5}$$

Where $P_{G,T}$ is the theoretical output power generated by the GCPV system at specific G (irradiance) and T (module temperature) values, n is the number of PV modules, $V_{G,T}$ is the theoretical output voltage generated by the GCPV system at specific G (irradiance) and T (module temperature) values and both V_0, P_o are the maximum operating voltage and power at STC (G: 1000 W/m^2, T: 25 °C) respectively.

The number of faulty PV modules can be expressed by the number of PV modules in the examined PV string. For example, if the PV string comprises 5 photovoltaic modules connected in series, then, n = 5.

In reality, the internal sensors used to measure the voltage and current for a GCPV system have efficiencies of less than 100%. This tolerance rate must therefore be considered in the PR and VR ratio calculations. For this instance, the PR and VR values are divided into two limits:

1. High limit: where the maximum operating efficiency of the sensors is applied, therefore, the high limit for both PR and VR ratios is expressed by (4) and (5).
2. Low limit: where the efficiency (tolerance rate) of the sensors is applied. Both limits can be expressed by the following formulas:

$$\text{PR Low limit} = \frac{P_{G,T}}{(P_{G,T} - nP_0)\eta_{sensor}} \tag{6}$$

$$\text{VR Low limit} = \frac{V_{G,T}}{(V_{G,T} - nV_0)\eta_{sensor1}} \tag{7}$$

Where η_{sensor} is the efficiency of both the voltage and current sensor, while, $\eta_{sensor1}$ is the efficiency of the voltage sensor:

$$\eta_{sensor} = \eta_{sensor1}(\text{Voltage Sensor efficiency}) + \eta_{sensor2}(\text{Current Sensor efficiency}) \tag{8}$$

The PR and VR high and low detection limits are evaluated for the examined GCPV system using various irradiance levels, as described in the third layer in Fig. 3. For this particular layer, the analysis of the PR vs. VR curves can be seen in the example shown next to layer 5, Fig. 3. This example shows the high and low detection limit for two case scenarios: one faulty PV module and two faulty PV modules, where both curves are created using 3rd order polynomial functions. The purpose of the 3rd order polynomial curves is to generate a regression function which describes the performance of the curves which are created by the theoretical points using VI LabVIEW software.

The overall GCPV fault detecting algorithm is explained in Fig. 3. Layer 5, shows the measured data vs. the 3rd order polynomial curves generated by VI LabVIEW software. The measured PR and measured VR can be evaluated using the following formula:

$$\text{Measured PR vs. Measured VR} = \frac{P_{G,T}}{P_{MEASURED}} \text{ vs. } \frac{V_{G,T}}{V_{MEASURED}} \tag{9}$$

In case of which the measured PR vs. VR is out of range:

$$\text{F High limit} < \text{Measured PR vs. Measured VR} < \text{F low limit}$$

Therefore, the fault detection algorithm cannot identify the type of the fault that has occurred in the GCPV plant. However, it can predict two possible faulty conditions which might have occurred in the GCPV system. As shown in Fig. 3, layer 5 example. The measured data 2 indicates two possible faulty conditions:

1. Faulty PV module and PS effects on the GCPV system
2. Two faulty PV modules and PS effects on the GCPV system

Therefore, out of region samples is processed by a fuzzy logic classifier as shown in Fig 3, layer 6.

The difference between the proposed theoretical curve modelling with other similar approaches described by [7, 8, 9 and 10] is that the algorithm contains the number of PV modules in the GCPV system, also the approach is using 3rd order polynomial function which can be used to plot a regression function that describes the behavior of the faulty region and the design of a fuzzy logic fault classification which is described in the next section (section 2.3).

2.3 Proposed Fault Detection Algorithm: Fuzzy Logic Classifier

Nowadays, fuzzy logic systems became more in use with PV systems. A brief overview of the recent publications on fuzzy logic system design is presented by L. Suganthi [27]. From the literature reviewed previously in the introduction, currently, there are a lack of research in the field of fuzzy logic classification systems which are used in examining faulty conditions in PV plants. Therefore, in this paper, a fuzzy logic classifier is demonstrated and verified experimentally.

Fig. 4 describes the overall fuzzy logic classifier system design. The fuzzy logic system consists of two inputs: voltage ratio (VR) and the power ratio (PR), denoted in Fig. 4 as (A) and (B) respectively. The membership function for each input is divided into five fuzzy sets described as: PS (partial shading condition), 1 (one faulty PV module), 2 (two faulty PV modules), 3 (three faulty PV modules) and 4 (four faulty PV modules). The fuzzy interface applies the approach of Mamdani method (min-max) managed by the fuzzy logic system rule, stage 2 of the fuzzy logic system. After the rules application, the output is applied to classify the fault detection type occurred in the GCPV plant.

A brief calculation of each membership function for VR, PR and the fuzzy logic membership output function is reported in Fig. 5. The membership functions are based on the mathematical calculation of the examined GCPV plant used in this work. The examined GCPV system which is used to evaluate the performance of the fault detection algorithm is demonstrated briefly in section 3.1: experimental setup. Both fuzzy logic system inputs VR and PR are evaluated at the maximum power and voltage of the GCPV system which are equal to 1100Wp and 143.5V. In addition, the mathematical calculations includes the PS conditions which might affect the performance of the entire PV system.

The fuzzy logic system rule are based on: if, and statement. Each case scenario is presented after the fuzzy logic system rule as shown in Fig. 5. However, the output membership function is divided into 5 sets: PS (0 - 0.2), faulty PV module (0.2 – 0.4), two faulty PV modules (0.4 – 0.6), three faulty PV modules (0.6 – 0.8) and four faulty PV modules (0.8 – 1.0).

Furthermore, the output surface for the fuzzy logic classifier system is plotted and presented by a 3D fitting curve shown in Fig. 6. Where the x-axis presents the PR, y-axis presents VR and the fault detection output classification is on the z-axis.

In order to generalize the proposed fuzzy logic classification systems, it is required to input the values of the voltage and the power to the fuzzy interface system, and then, the faulty region could be calculated using the formulas (4 & 5) for the variations of the power and voltage respectively. Additionally, the output detection membership function could be extended up to the value of the PV modules connected in series in each PV string separately and this extension in the membership function can be evaluated within the region of 0 to 1 as the following:

$$1 \,/\, \text{number of series PV modules in the PV string}$$

3. GCPV Fault Detection Algorithm Validation

In this section, the performance of the proposed fault detection algorithm is verified. For this purpose, the acquired data for various days have been considered using 1.1 kWp GCPV plant. The time zone for all measurements is GMT.

3.1 Experimental Setup

The PV system used in this work consists of a GCPV plant comprising 5 polycrystalline silicon PV modules each with a nominal power of 220 Wp. The PV modules are connected in series. The PV string is connected to a Maximum Power Point Tracker (MPPT) with an output efficiency of not less than 95%. The DC current and voltage are measured using the internal sensors which are part of the FLEXmax MPPT unit. A battery bank is used to store the energy produced by the PV plant.

A Vantage Pro monitoring unit is used to receive the Global solar irradiance measured by the Davis weather station which includes a pyranometer. A Hub 4 communication manager is used to facilitate acquisition of modules' temperature using the Davis external temperature sensor, and the electrical data for each PV string. VI LabVIEW software is used to implement data logging and monitoring functions of the GCPV system. Fig. 7 illustrates the overall system architecture of the GCPV plant.

The real-time measurements are taken by averaging 60 samples, gathered at a rate of 1Hz over a period of one minute. Therefore, the obtained results for power, voltage and current are calculated at one minute intervals.

The SMT6 (60) P solar module manufactured by Romag, has been used in this work. The electrical characteristics of the solar module are shown in Table 1. The standard test condition (STC) for these solar panels are: Solar Irradiance = 1000 W/m^2, Module Temperature = 25 °C.

The fault detection algorithm has been validated experimentally over a 5 day period. On each day a different fault case scenario was perturbed as shown in Fig. 8:

1. Day1: Normal operation mode and PS effects on the GCPV plant (no fault occurred in any of the tested PV modules),
2. Day2: One faulty PV module and PS effects on the GCPV plant
3. Day3: Two faulty PV modules and PS effects on the GCPV plant
4. Day4: Three faulty PV modules and PS effects on the GCPV plant
5. Day5: Four faulty PV modules and PS effects on the GCPV plant

In all cases, faulty PV module stands for an in active PV module which means that this particular PV module has been disconnected (short circuit) from the entire examined PV plant.

In order to test the effectiveness of the proposed fault detection algorithm, the theoretical and the measured output power for each case scenario was logged and compared using VI LabVIEW software.

3.2 Evaluation of the Proposed Theoretical Curves Modelling

In this section, the performance of the fault detection algorithm (theoretical curves modelling) is verified using normal operation mode and partial shading effects the GCPV system. Fig. 9 describes the theoretical simulation vs. real time long term data measurement.

In order to apply a partial shading condition to the GPCV modules an opaque paper object has been used. The partial shading was applied to all PV modules at the same rate. Partial shading condition is increased during the test. In case of overcast scenario affecting the PV modules, the performance of the entire system will remain with a consistent output power, therefore, the faults or PS conditions could be identified using the purposed algorithm.

Fig. 10(A) shows the entire measured data vs. theoretical detection limits which are discussed previously in section 2.2. As can be noticed, most of the measured data lies within the high and low theoretical detection limits which are created using 3rd order polynomial function. The high and low detection limit functions are also illustrated in the Fig 10(A).

PR and VR ratios for this particular test is shown in Fig 10(B). Since the PS condition applied to the GCPV system is increasing, therefore, both VR and PR ratios are increasing slightly during the test. Moreover, both ratios can be measured using (9). Fig. 10(B) shows the efficiency of the GCPV plant. The efficiency is evaluated using (10).

$$\text{Efficicnecy} = \frac{\text{Measured Output Power}}{\text{Theoretical Power}} \tag{10}$$

From Fig. 10(B), the efficiency of the GCPV system decreased while increasing the PS applied to the PV system. The detection accuracy (DA) for the proposed theoretical curves modelling algorithm is calculated using (11).

$$\text{Detection accuracy (DA)} = \frac{\text{Total Number of Samples} - \text{Out of Region Samples}}{\text{Total Number of Samples}} \tag{11}$$

Using (11), the proposed algorithm has a detection accuracy equals to:

$$\text{Detection accuracy for the partial shading condtion} = \frac{720 - 37}{720} = 0.9486 = 94.86\%$$

In this test, the theoretical curves modelling fault detection algorithm shows a significant success for detecting partial shading conditions applied to the GCPV plant. The detection accuracy rate can be increased using a fuzzy logic classification system. Therefore, out of region samples (samples which are away from the high and low detection limits) are processed by the fuzzy logic system.

In this paper, the MPPT unit is used to locate and acquired the output power at the global maximum power point (GMPP), therefore, all local maximum power points (LMPP) are not considered in the fault detection algorithm. Fig. 11(A) illustrates one examined case scenario which shows the percentage of the partial shading on each examined PV module. The output P-V curve of the PV system is shown in Fig. 11(B). As can be noticed, the MPPT unit locates all LMPP and GMPP, however, the output of the MPPT unit is at the GMPP.

In order to detect all LMPPs and the GMPP obtained by the MPPT unit, it is required to further investigate MPPT techniques which is not one of the targets of this manuscript.

3.3 Evaluation of the Proposed Fuzzy Logic Classification System

This test is created to confirm the ability of the fault detection algorithm to detect faulty PV modules occurring in the GCPV plant using theoretical curves modelling algorithm and fuzzy logic classification system. Four different case scenarios have been tested:

A. Faulty PV module with partial shading condition
B. Two faulty PV modules with partial shading condition
C. Three faulty PV modules with partial shading condition
D. Four faulty PV module and partial shading condition

Each case scenario is examined during a time period of a full day as shown Fig. 8 (Day 2, 3, 4 and 5), where the total number of samples for each examined day are equal to 720 samples. Fig. 10 shows the theoretical curve limits vs. real-time long-term measured data. 3rd order polynomial function of the theoretical high and low limits is plotted, while the minimum determination factor (R) is equal to 99.59%.

As can be noticed, the measured data for each test is plotted and compared with the theoretical curve limits. Most of the measured data among the 4 day test period lies within the high and low detection limits of the theoretical curves. However, in each day, several out of region samples have been detected as shown in Fig. 12.

The detection accuracy (DA) for each case scenario is calculated using (11) and reported in Table 2. The minimum and maximum DA is equal to 94.03% and 95.27% respectively before considering the fuzzy logic classification system.

For each test including the test illustrated in section 3.2, out of region samples have been processed by the fuzzy logic classification system. Fig. 13 describes the performance of the fuzzy logic system during each test:

- Test 1: PS, described in section 3.2
- Test 2: One faulty PV module and PS
- Test 3: Two faulty PV modules and PS
- Test 4: Three faulty PV modules and PS
- Test 5: Four faulty PV modules and PS

It is evident that most of the samples are categorized correctly by the fuzzy classifier. For example, before considering the fuzzy logic system, the DA for test 2 is equal to 95.27% while the DA increased up to 99.03% after taking into account the fuzzy logic classification system. This result is due to the detection of the out of region samples. The results for this test is shown in Fig. 13, only 7 out of 34 processed samples are detected incorrectly, while 27 samples have been detected correctly within an output membership function between 0.2 and 0.4.

Table 2 shows number of out of region samples and the detection accuracy (DA) for each test separately. The DA rate is increased up to a minimum value equals to 98.8%.

In this section, the evaluation for the theoretical curves modelling algorithm and the fuzzy logic system are discussed and briefly explained. From the obtained results, it is confirmed that the fault detection algorithm proposed in this article is suitable for detecting faulty conditions in PV systems accurately.

3.4 Evaluation of the Proposed Method Using Hot Spot Detection in PV Modules

This test is created to confirm the ability of the fault detection algorithm to detect hot spots in PV modules. The test was evaluated using two different PV modules which contains different hot spots. As shows in Fig. 14(A), the first PV module contains only one hot spot in the top right side of the PV module, however, the second tested PV module contains two adjacent hot spots. The thermal images were taken from FLIR i7 camera, which has a thermal sensitivity equals to 0.1 ^{0}C (32.18 ^{0}F).

The first PV module temperature is measured at 55.4 ^{0}F, while the hot spot has been detected at 60.2 ^{0}F. Same results obtained for the second PV module where the PV module temperature is approximately equals to 56.8 ^{0}F. However, the hot spots detected in the PV module have a temperature equal to 59.6 ^{0}F and 62.3 ^{0}F.

The theoretical curves modelling was used to evaluate the difference between a healthy PV module (PV module without hot spots) with the examined PV modules shown in Fig. 14(A) at the same environmental conditions. The results of this test is shown in Fig. 14(B). As can be noticed, the detection limits of the theoretical curves does only contain most of the PV data obtained from the healthy PV module. Furthermore, the measured data of the first PV module which contains only one hot spot shows an increase in the values of the PR and VR. This results is due to the decrease in the value of the voltage obtained from the PV module. The voltage from this particular PV module is decreased approximately about 2V. Therefore the overall VR and PR is increased as can be demonstrated by (12).

The second PV module has more drop in the value of the voltage due to the detection of two hot spots. The drop in the value of the voltage is estimated at 3.7V. As shown in Fig. 14(B), the measured data obtained from the second PV module show a significant increase in the values of the VR and PR. Therefore, the measured data is apart from the detection limits obtained by the fault detection algorithm.

$$\uparrow \mathrm{VR} = \frac{\mathrm{V_{G,T\ theoretical}}}{\downarrow \mathrm{V_{G,T\ measured}} - \mathrm{nV_0}} \quad \& \quad \uparrow \mathrm{PR} = \frac{\mathrm{P_{G,T\ theoretical}}}{\downarrow \mathrm{P_{G,T\ measured}} - \mathrm{nP_0}} \tag{12}$$

3.5 Discussion

In order to test the effectiveness of the proposed fault detection algorithm presented in this paper, the results obtained have been compared with multiple fault detection approaches. The common combination between the proposed algorithm in this paper and the research demonstrated by [5, 8 and 28] is the VR and PR equations. However, the VR and PR equations presented in this work have a different parameters such as:

1. VR and PR equations contain the number of modules that are examined in the GCPV plant, which is presented using the variable: n.
2. Both equations contain the voltage and current sensors uncertainly (sensor efficiency rate), which makes the algorithm easier to use with different PV installations.
3. The detection limits (high and low) is a novel idea which has not been presented by any other research article related to fault detection algorithms in PV systems.

Moreover, by using VR and PR ratios it was evident that the algorithm can detect up to (n-1) faulty PV modules and PS effects the GCPV plant, where n is equal to the number of PV modules in the examined GCPV installation. In this paper, a MPPT unit which has an output power of one single point (mostly, it is

equal to the GMPP), therefore, the detection algorithm is not capable of detecting and categorizing ALL LMPP, since the examined PV system is using a MPPT unit without any enhancement of the output power using an advanced MPPT techniques.

In [7 and 12] statistical analysis technique based on standard divination limits are used to detect possible faults in the GCPV plant, however, the presented techniques cannot identify the type of the fault occurred in the PV system, therefore, it is necessary to create a new mathematical calculations of the entire GCPV plant. In this paper, it is presented that the algorithm is based on the analysis of the theoretical curves modelling using 3rd order polynomial functions, without the use of any statistical analysis approaches.

Furthermore, [10] experimented another statistical analysis technique called t-test. This algorithm is capable to detect multiple faults in PV systems, however, the ratios used to monitor the performance of the PV system does not contain any parameter for the number of PV modules and the uncertainly in the internal voltage and current sensors used.

There are variety of fuzzy logic control systems used with PV applications. Three-phase three-level grid interactive inverter with fuzzy based maximum power point tracking controller is presented by [29]. Additionally, some of the fuzzy logic classification systems were used with hybrid green power systems as reported by S. Safari et al [30]. Furthermore, M. Tadj et al [5] presented a fuzzy logic technique which is used to estimate the solar radiation, the proposed technique contains three membership functions: cloudy sky, partial cloudy sky and clear sky. However, in this paper, a new attempt for using fuzzy logic classification system to detect possible faults occurring in the PV plans. The main purpose of the fuzzy logic presented in this work is to detect out of region samples (samples that lies away from the high and low theoretical detection limits), and therefore, to increase the detection accuracy of the fault detection algorithm. The fuzzy logic system can be reused with other GCPV plants by changing the parameters which are shown in Fig. 5.

Overall comparison between this work and the research presented by [4, 7 & 8] are listed in Table 3. As can be seen that this work is the only research contains a mathematical modelling technique (3rd order polynomial functions) presented previously in Layer 3, Fig 3. Also this paper demonstrates a new statistical technique which can be used in the detection of faulty conditions in PV systems called t-test statistical method. Comparing to [4, 7 and 8], the proposed fault detection algorithm presented in this research can detects all type of faults listed in Table 3 including: partial shading conditions, faulty PV modules and evaluating the hot spots in PV modules. However, the algorithm cannot distinguish between the investigated partial shading conditions occurred in the PV modules and hot spots.

The fault detection algorithm presented in this work contains some advantages and disadvantages such as:

Advantages:

- The fault detection algorithm can be used with wide range of PV installation, since it depends on the analysis of the power and the voltage ratios.
- Multiple faults can be detected accurately, the minimum and maximum detection accuracy obtained by the algorithm are equal to 98.8% and 99.31% respectively.
- The efficiency of the voltage and current sensor has been taken into account in the mathematical modelling for the proposed fault detection algorithm.
- The fuzzy logic classification system is easy to be reused in other PV systems since it depends only on the analysis of the VR and PR.
- Hot spot detection can also be evaluated using the proposed theoretical curves modelling.

Disadvantages:

- The algorithm depends on the voltage and the power ratios of the GCPV systems. Therefore, the accuracy of the algorithm depends on the instrumentation used in the PV plants.
- The algorithm is not capable of detecting faults occurring in the bypass diodes, which are commonly used nowadays with PV systems. This problem in GCPV plants has been investigated by W. Chine [9].
- The fault detection algorithm cannot detect any fault arising in the DC/AC inverter units which are commonly used with GCPV systems. This type of fault has been reported by R. Platon et al [12], G. Bayrak [23] and F. Deng et al [31].

4. Conclusion

In this work, a new GCPV fault detection algorithm is proposed. The developed fault detection algorithm is capable of detecting faulty PV modules and partial shading conditions which affect GCPV systems. The detection algorithm has been tested using 1.1kWp GCPV system installed at Huddersfield University, United Kingdom.

The fault detection algorithm consist of six layers working in series. The first layer contains the input parameters of the sun irradiance and PV modules' temperature, while the second layer generates the GCPV theoretical performance analysis using Virtual Instrumentation (VI) LabVIEW software. Layer 3 identifies the power and voltage ratios, subsequently creates a high and low detection limits which will be used in Layer 4 to apply the 3rd order polynomial regression model on the top of the PR and VR ratios. The fifth layer consists of two parts: the input parameters of the examined GCPV systems and the 3rd order polynomial detection limits. If the measured voltage ratio vs. measured power ratio lies away from the detection limits, the samples will be processed by the last layer which contains the fuzzy logic classification system.

The novel contribution of this research is that the fault detection algorithm depends on the variations of the voltage and the power of the GCPV plant. Additionally, the PR and VR equations contains the number of examined modules and the uncertainly of the voltage and current sensors used. Also, there are a few fuzzy logic classification systems which are used with PV fault detection algorithms, therefore, this research introduced a simple, reliable and quick fuzzy logic classification system which can be reused with various GCPV plants. Finally, the PV theoretical curves modelling can be used to evaluate PV modules which contain hot spots.

The results indicate that the fault detection algorithm is detecting most of the measured data within the theoretical limits created using 3rd order polynomial functions. Furthermore, the maximum detection accuracy of the algorithm before considering the fuzzy logic system is equal to 95.27%, however, the fault detection accuracy is increased up to a minimum value of 98.8% after considering the fuzzy logic system.

In future, it is intended to implement the proposed fault detection technique on a low cost microcontroller based system. The system's fault detection capabilities will be enhanced further by using artificial intelligence machine learning technique to predict possible faults occurring in the GCPV system using artificial neural networks (ANN).

5. *Acknowledgment*

The authors would like to acknowledge the financial support to the University of Huddersfield, School of Computing and Engineering.

References

[1] Bortolini, M., Gamberi, M., & Graziani, A. (2014). Technical and economic design of photovoltaic and battery energy storage system. *Energy Conversion and Management*, *86*, 81-92.

[2] Dhimish, M., Holmes, V., Mehrdadi, B., Dales, M., Chong, B., & Zhang, L. (2017). Seven indicators variations for multiple PV array configurations under partial shading and faulty PV conditions. *Renewable Energy*.

[3] Kadri, R., Andrei, H., Gaubert, J. P., Ivanovici, T., Champenois, G., & Andrei, P. (2012). Modeling of the photovoltaic cell circuit parameters for optimum connection model and real-time emulator with partial shadow conditions. *Energy*, *42*(1), 57-67.

[4] Dhimish, M., Holmes, V., Mehrdadi, B., & Dales, M. (2017). Diagnostic method for photovoltaic systems based on six layer detection algorithm. *Electric Power Systems Research*, *151*, 26-39.

[5] Tadj, M., Benmouiza, K., Cheknane, A., & Silvestre, S. (2014). Improving the performance of PV systems by faults detection using GISTEL approach. *Energy conversion and management*, *80*, 298-304.

[6] Takashima, T., Yamaguchi, J., Otani, K., Oozeki, T., Kato, K., & Ishida, M. (2009). Experimental studies of fault location in PV module strings. *Solar Energy Materials and Solar Cells*, *93*(6), 1079-1082.

[7] Chouder, A., & Silvestre, S. (2010). Automatic supervision and fault detection of PV systems based on power losses analysis. *Energy Conversion and Management*, *51*(10), 1929-1937.

[8] Silvestre, S., Kichou, S., Chouder, A., Nofuentes, G., & Karatepe, E. (2015). Analysis of current and voltage indicators in grid connected PV (photovoltaic) systems working in faulty and partial shading conditions. *Energy*, *86*, 42-50.

[9] Chine, W., Mellit, A., Lughi, V., Malek, A., Sulligoi, G., & Pavan, A. M. (2016). A novel fault diagnosis technique for photovoltaic systems based on artificial neural networks. *Renewable Energy*, *90*, 501-512.

[10] Dhimish, M., & Holmes, V. (2016). Fault detection algorithm for grid-connected photovoltaic plants. *Solar Energy*, *137*, 236-245.

[11] Dhimish, M., Holmes, V., Mehrdadi, B., & Dales, M. (2017). Multi-Layer Photovoltaic Fault Detection Algorithm. *High Voltage*.

[12] Platon, R., Martel, J., Woodruff, N., & Chau, T. Y. (2015). Online Fault Detection in PV Systems. *IEEE Transactions on Sustainable Energy*, *6*(4), 1200-1207.

[13] Kim, K. A., Seo, G. S., Cho, B. H., & Krein, P. T. (2016). Photovoltaic Hot-Spot Detection for Solar Panel Substrings Using AC Parameter Characterization. *IEEE Transactions on Power Electronics*, *31*(2), 1121-1130.

[14] Dhimish, M., Holmes, V., Mehrdadi, B., & Dales, M. (2017). The Impact of Cracks on Photovoltaic Power Performance. *Journal of Science: Advanced Materials and Devices*.

[15] Obi, M., & Bass, R. (2016). Trends and challenges of grid-connected photovoltaic systems–A review. *Renewable and Sustainable Energy Reviews*, *58*, 1082-1094.

[16] Alam, M. K., Khan, F., Johnson, J., & Flicker, J. (2015). A Comprehensive Review of Catastrophic Faults in PV Arrays: Types, Detection, and Mitigation Techniques. *IEEE Journal of Photovoltaics*, *5*(3), 982-997.

[17] Khamis, A., Shareef, H., Bizkevelci, E., & Khatib, T. (2013). A review of islanding detection techniques for renewable distributed generation systems. *Renewable and sustainable energy reviews*, *28*, 483-493.

[18] Boukenoui, R., Salhi, H., Bradai, R., & Mellit, A. (2016). A new intelligent MPPT method for stand-alone photovoltaic systems operating under fast transient variations of shading patterns. *Solar Energy*, *124*, 124-142.

[19] Mutlag, A. H., Shareef, H., Mohamed, A., Hannan, M. A., & Abd Ali, J. (2014). An improved fuzzy logic controller design for PV inverters utilizing differential search optimization. *International Journal of Photoenergy*, *2014*.

[20] Belaout, A., Krim, F., & Mellit, A. (2016, November). Neuro-fuzzy classifier for fault detection and classification in photovoltaic module. In *Modelling, Identification and Control (ICMIC), 2016 8th International Conference on* (pp. 144-149). IEEE.

[21] Grichting, B., Goette, J., & Jacomet, M. (2015, June). Cascaded fuzzy logic based arc fault detection in photovoltaic applications. In *Clean Electrical Power (ICCEP), 2015 International Conference on* (pp. 178-183). IEEE.

[22] Chen, J. L., Kuo, C. L., Chen, S. J., Kao, C. C., Zhan, T. S., Lin, C. H., & Chen, Y. S. (2016). DC-Side Fault Detection for Photovoltaic Energy Conversion System Using Fractional-Order Dynamic-Error-based Fuzzy Petri Net Integrated with Intelligent Meters. *IET Renewable Power Generation*.

[23] Bayrak, G. (2015). A remote islanding detection and control strategy for photovoltaic-based distributed generation systems. *Energy Conversion and Management*, *96*, 228-241.

[24] Dhimish, M., Holmes, V., & Dales, M. (2017). Parallel fault detection algorithm for grid-connected photovoltaic plants. *Renewable Energy*, *113*, 94-111.

[25] McEvoy, A., Castaner, L., Markvart, T., 2012. Solar Cells: Materials, Manufacture and Operation. Academic Press.

[26] Sera, D., Teodorescu, R., & Rodriguez, P. (2007). PV panel model based on datasheet values. Paper presented at the 2392-2396. doi:10.1109/ISIE.2007.4374981

[27] Suganthi, L., Iniyan, S., & Samuel, A. A. (2015). Applications of fuzzy logic in renewable energy systems–a review. *Renewable and Sustainable Energy Reviews*, *48*, 585-607.

[28] Chine, W., Mellit, A., Pavan, A. M., & Kalogirou, S. A. (2014). Fault detection method for grid-connected photovoltaic plants. *Renewable Energy*, *66*, 99-110.

[29] Altin, N., & Ozdemir, S. (2013). Three-phase three-level grid interactive inverter with fuzzy logic based maximum power point tracking controller. *Energy Conversion and Management*, *69*, 17-26.

[30] Safari, S., Ardehali, M. M., & Sirizi, M. J. (2013). Particle swarm optimization based fuzzy logic controller for autonomous green power energy system with hydrogen storage. *Energy conversion and management*, *65*, 41-49.

[31] Deng, F., Chen, Z., Khan, M. R., & Zhu, R. (2015). Fault detection and localization method for modular multilevel converters. *IEEE Transactions on Power Electronics*, *30*(5), 2721-2732.

518 ***List of Figures:***

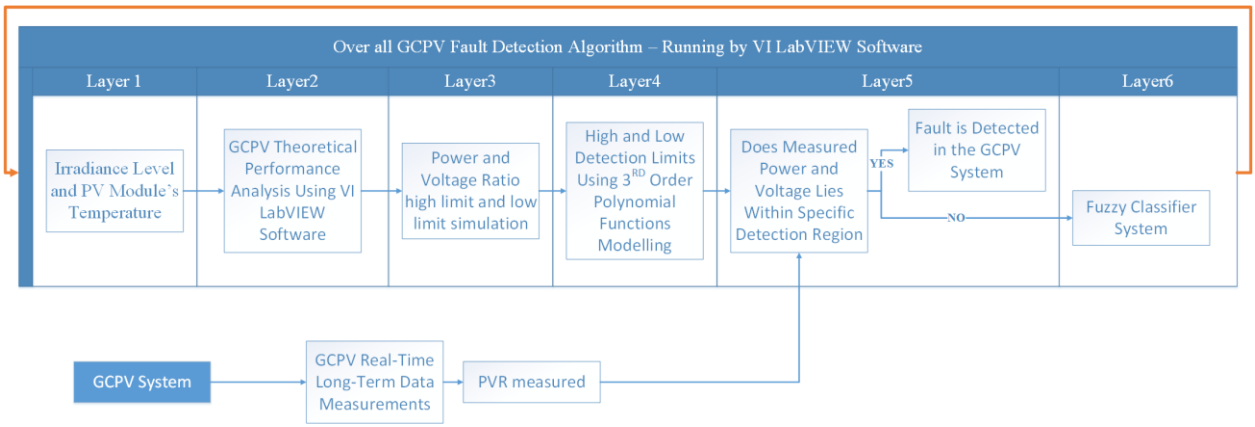

Fig. 1. Over all GCPV fault detection algorithm Layers

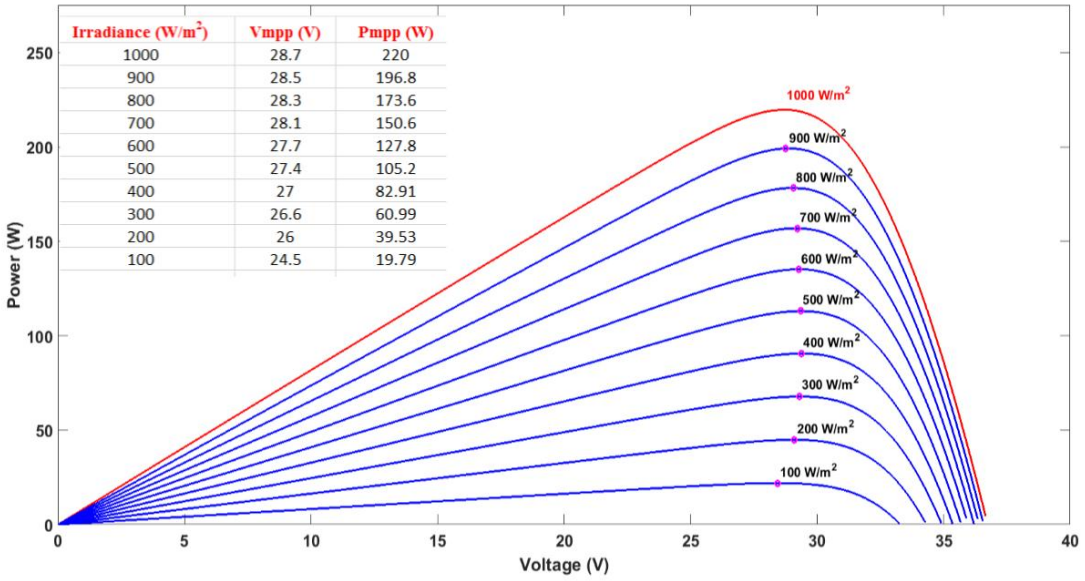

Fig. 2. P-V curve modelling under various irradiance levels

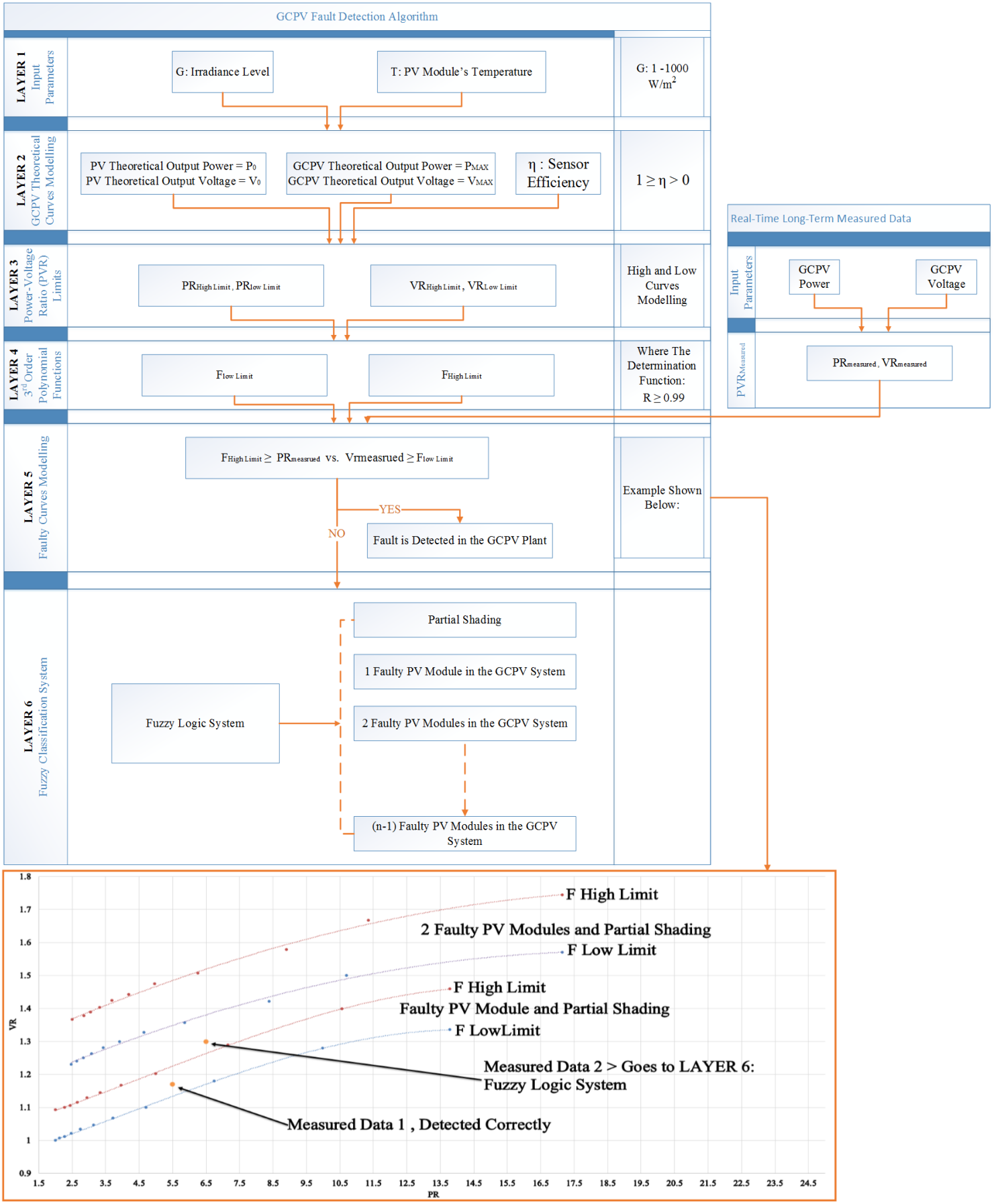

Fig. 3. Detailed flowchart for the proposed fault detection algorithm which contains 5 layers

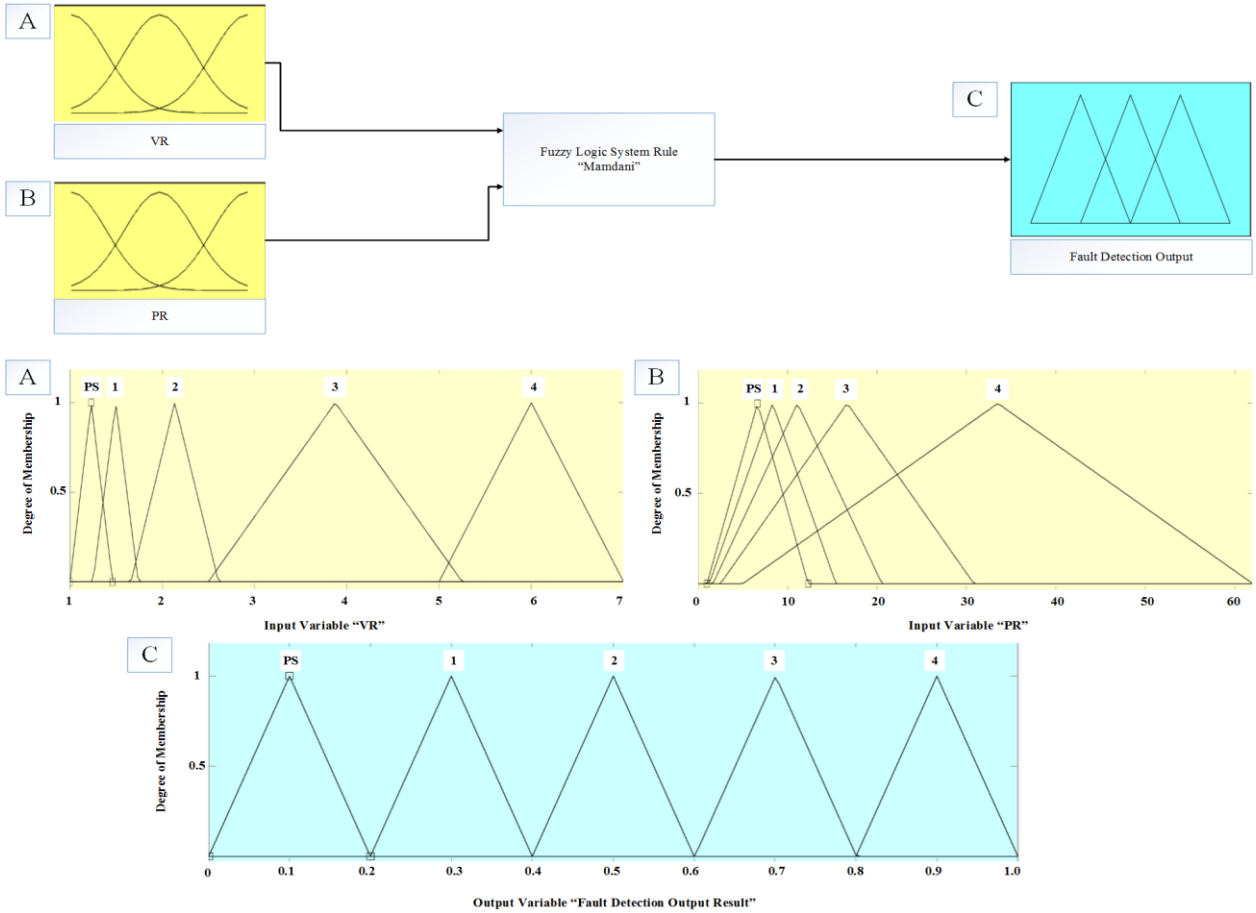

Fig. 4. Fuzzy Logic classifier system design. (A) Voltage ratio input, (B) Power ratio input, (C) Fault detection output

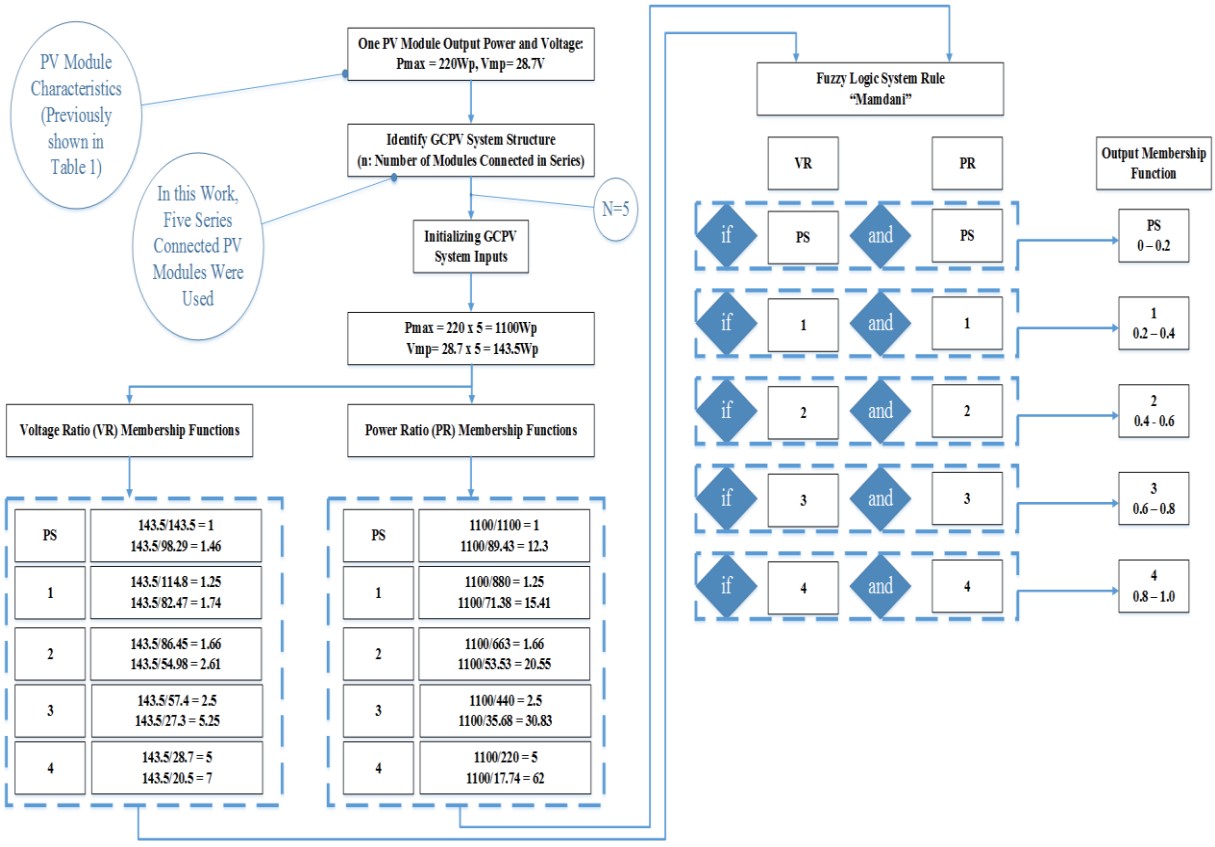

Fig. 5. Mathematical calculations for the fuzzy logic classifier system including VR, PR, Rules and Output Membership Function

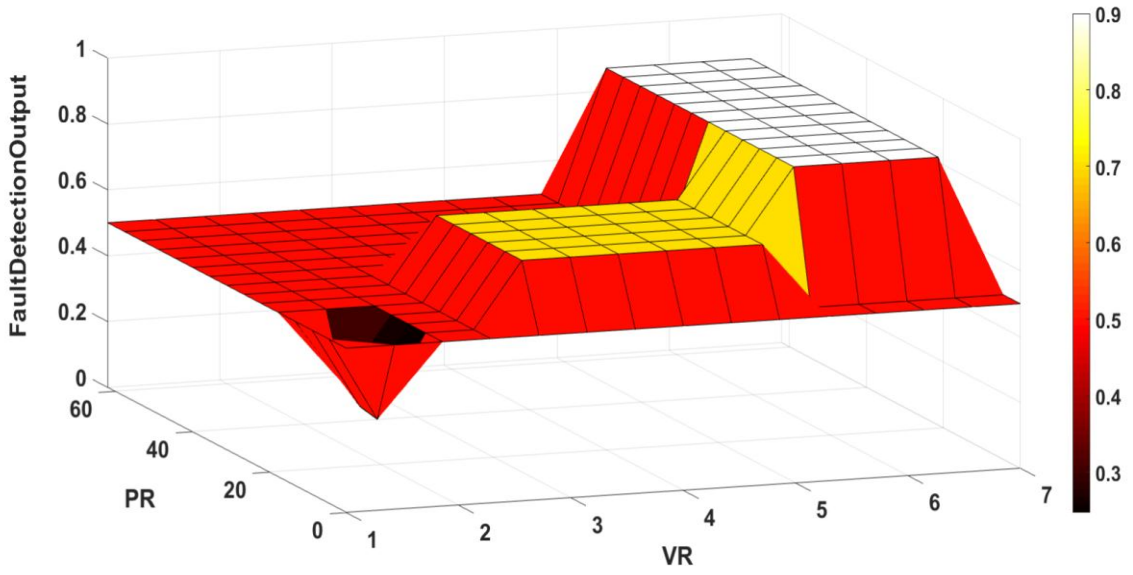

Fig. 6. Fuzzy Logic classifier output surface with VR, PR and the fault detection output membership function

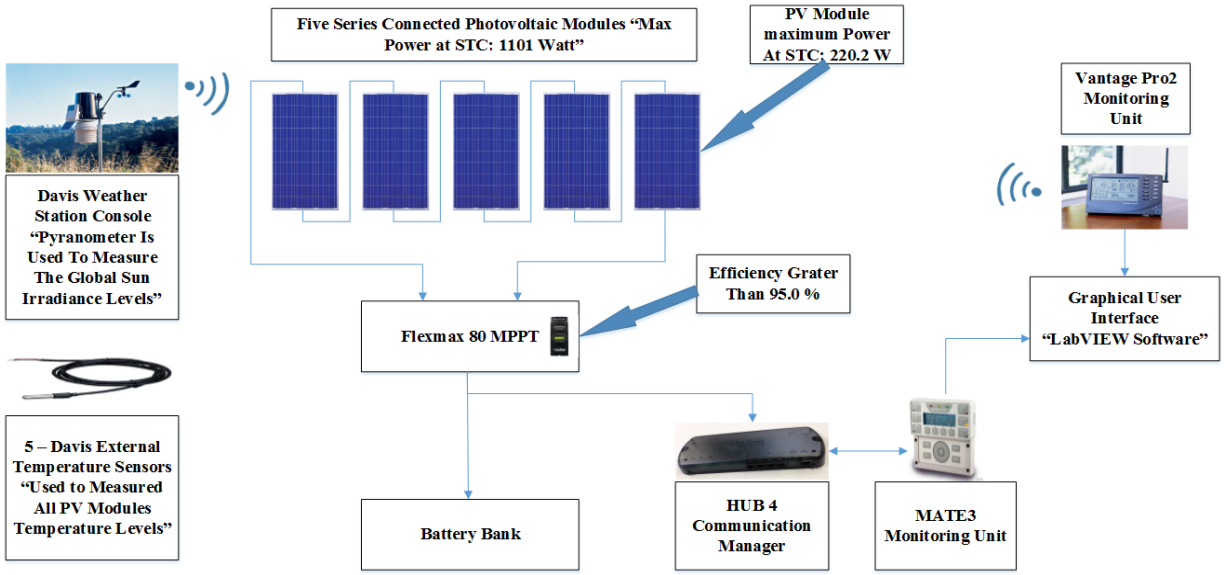

Fig. 7. Examined GCPV Plant Installed at the Huddersfield University, United Kingdom

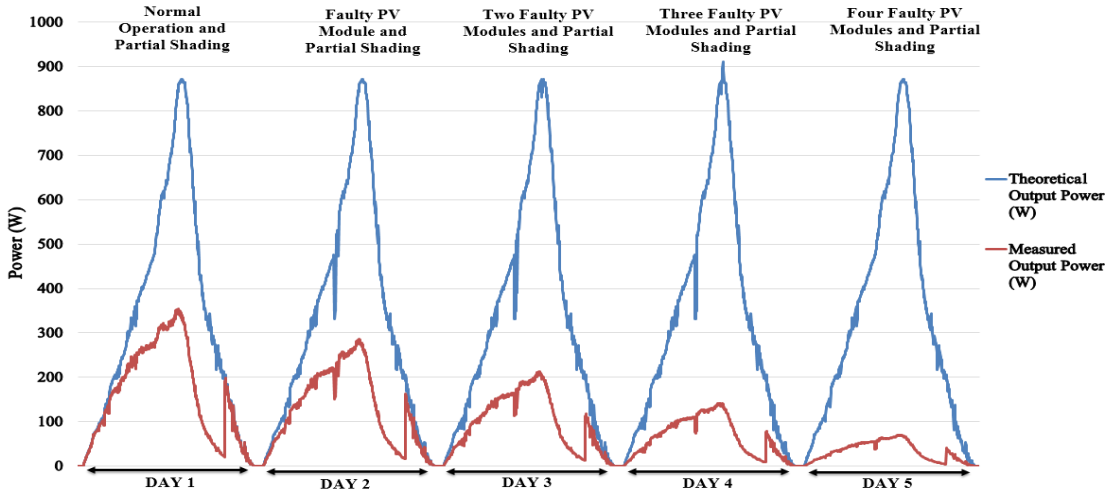

Fig. 8. Theoretical vs. Measured output power during 5 different days

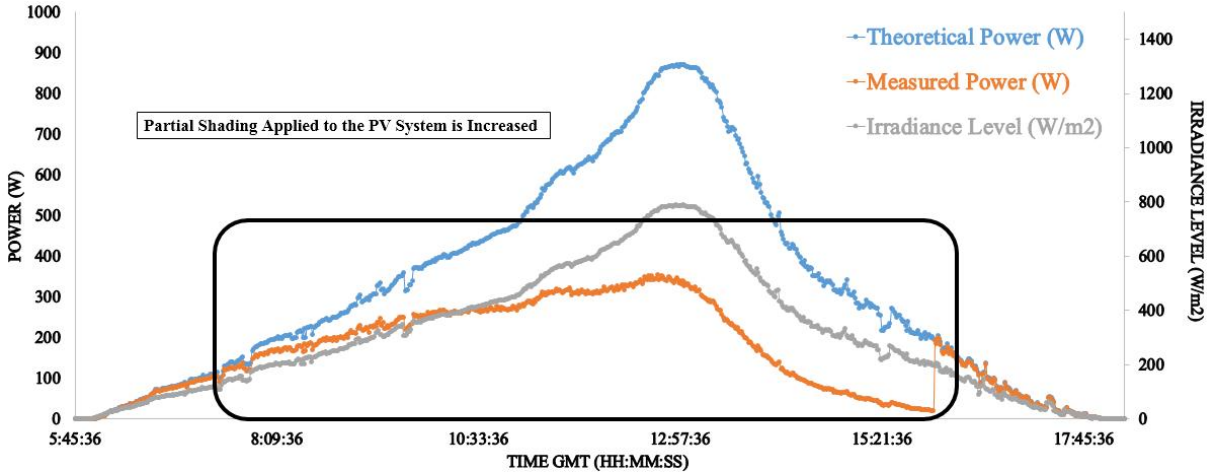

Fig. 9. Theoretical power vs. measured output power for a partial shading effects the GCPV plant

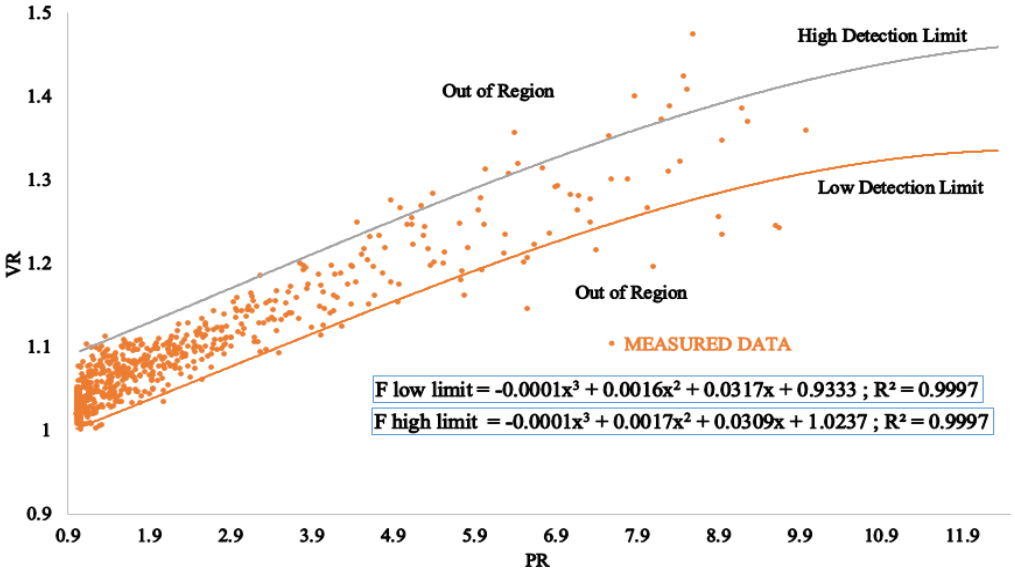

(A)

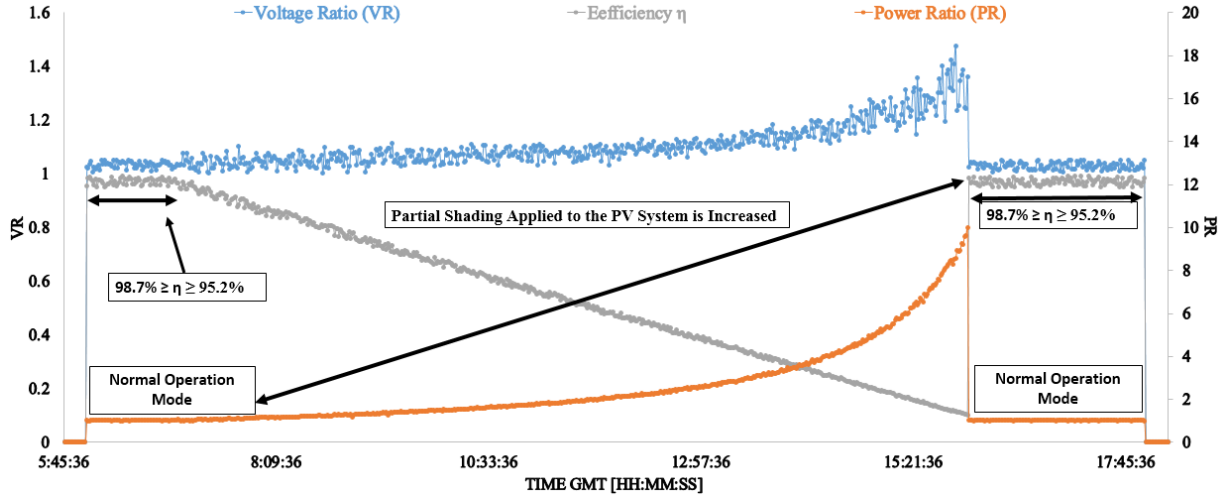

(B)

Fig. 10. Theoretical curves vs. real time long term measured data. (A) Theoretical fault curve detection limits for the examined GCPV plant, (B) Voltage ratio, power ratio and the efficiency of the entire GCPV system

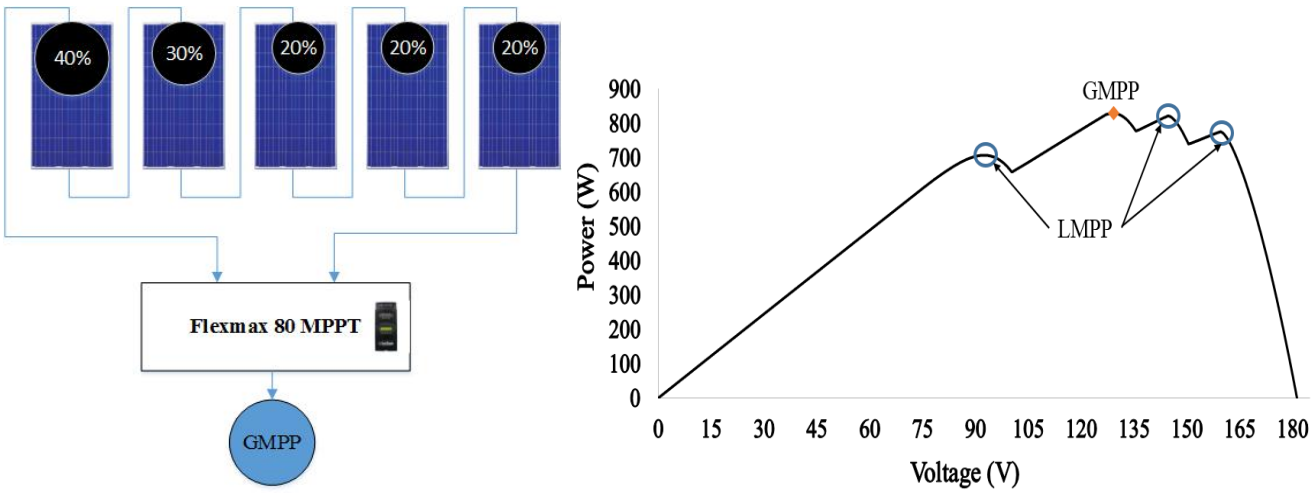

(A) (B)

Fig. 11. MPPT unit output power (A) Examined partial shading condition, (B) P-V curve including the output LMPP and GMPP obtained by the MPPT unit

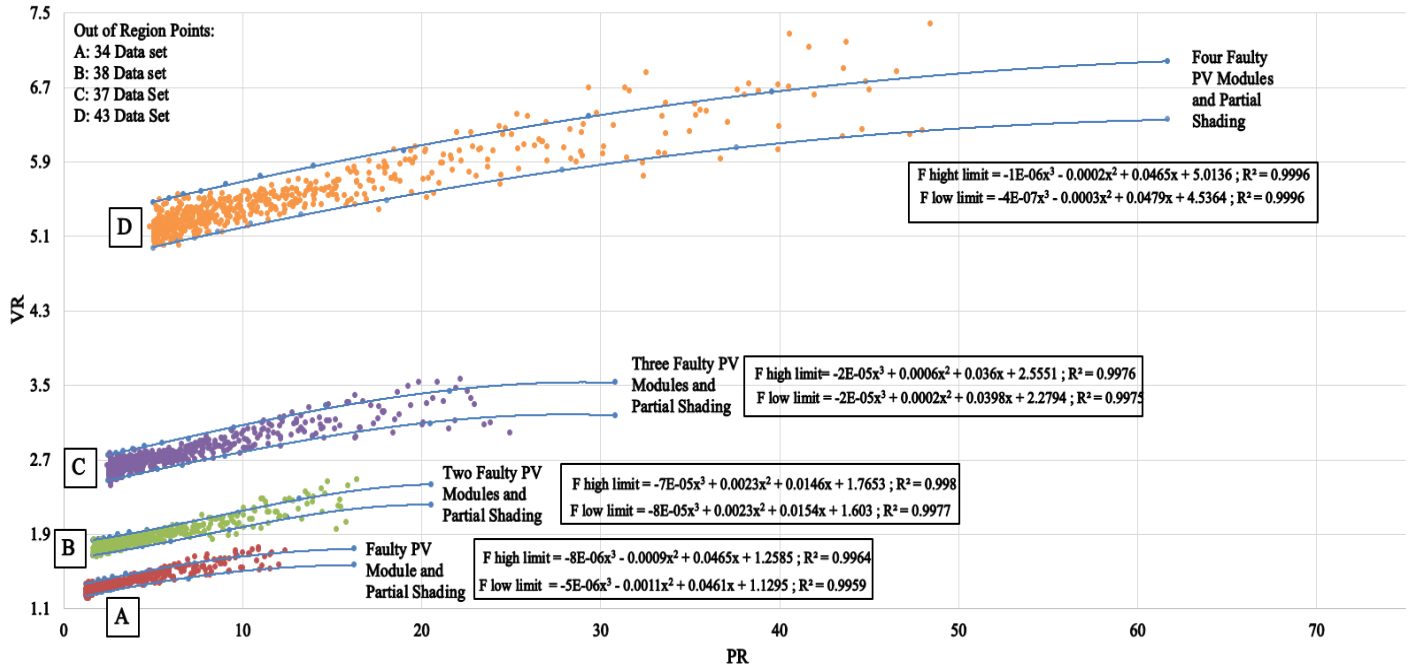

Fig. 12. Theoretical detection limits vs. real-time long-term data measurements for one faulty, two faulty, three faulty and four faulty photovoltaic modules

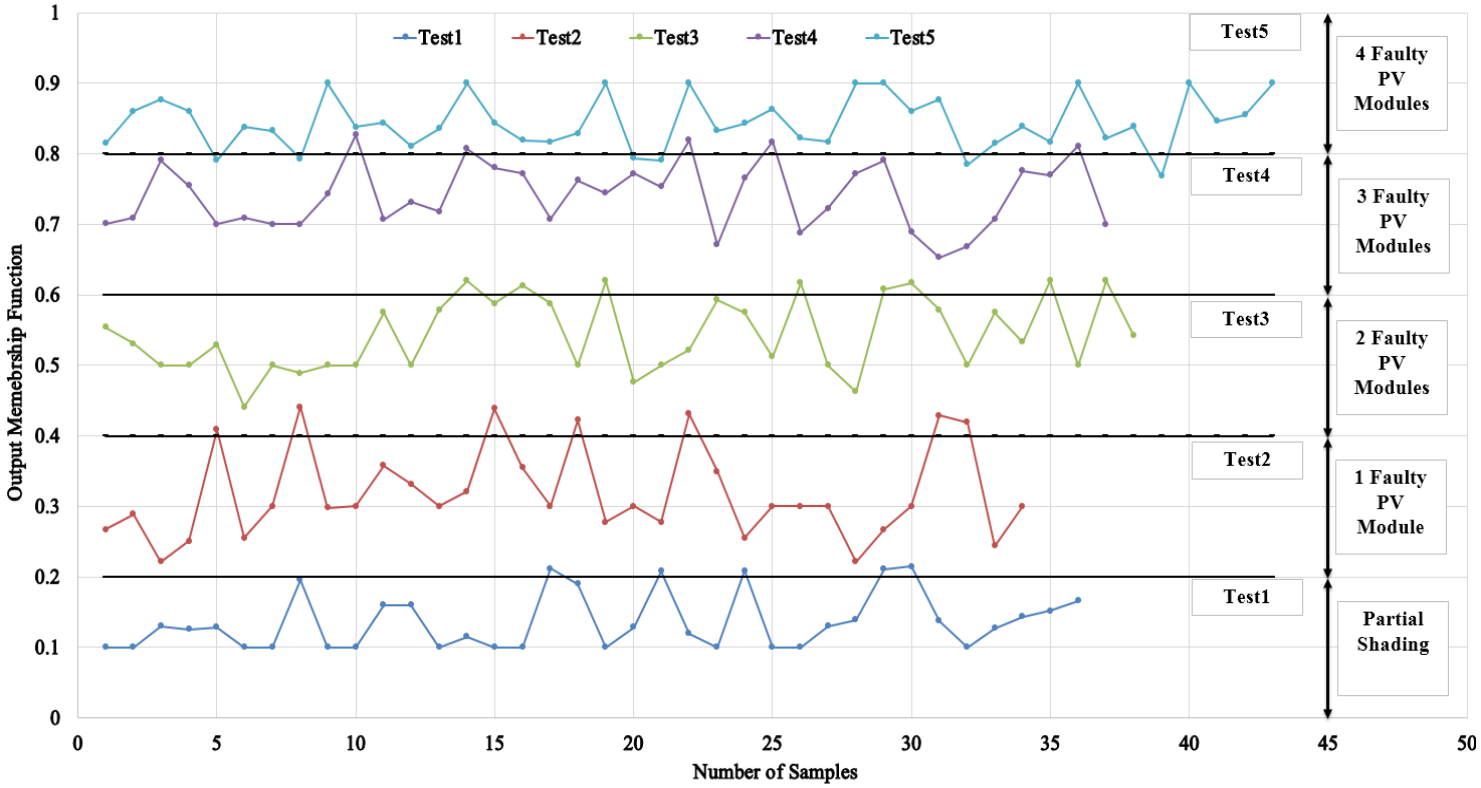

Fig. 13. Out of region samples processed by the fuzzy logic classification system

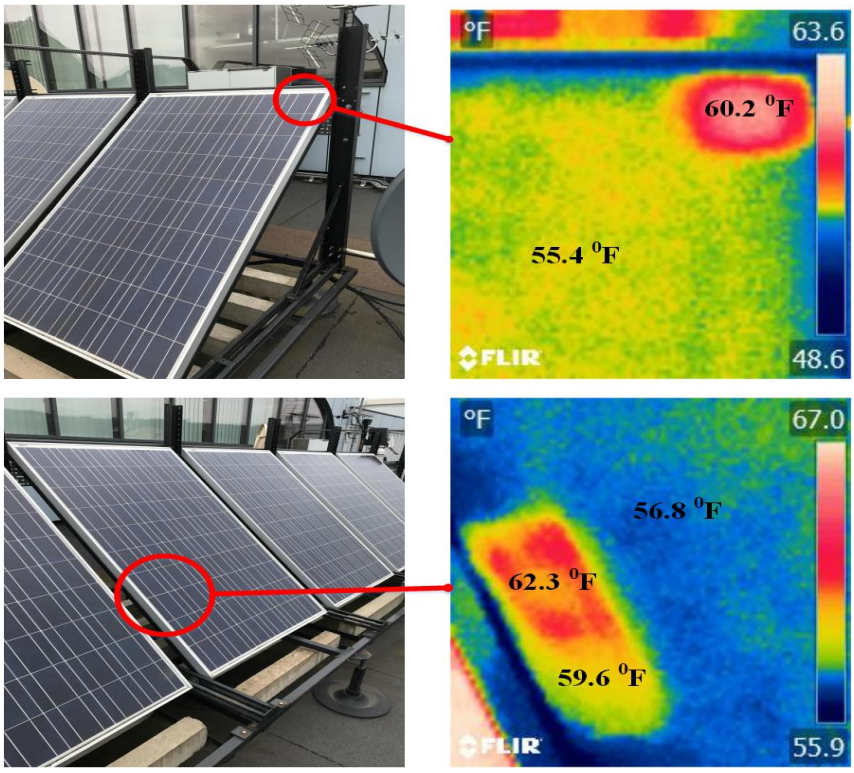

(A)

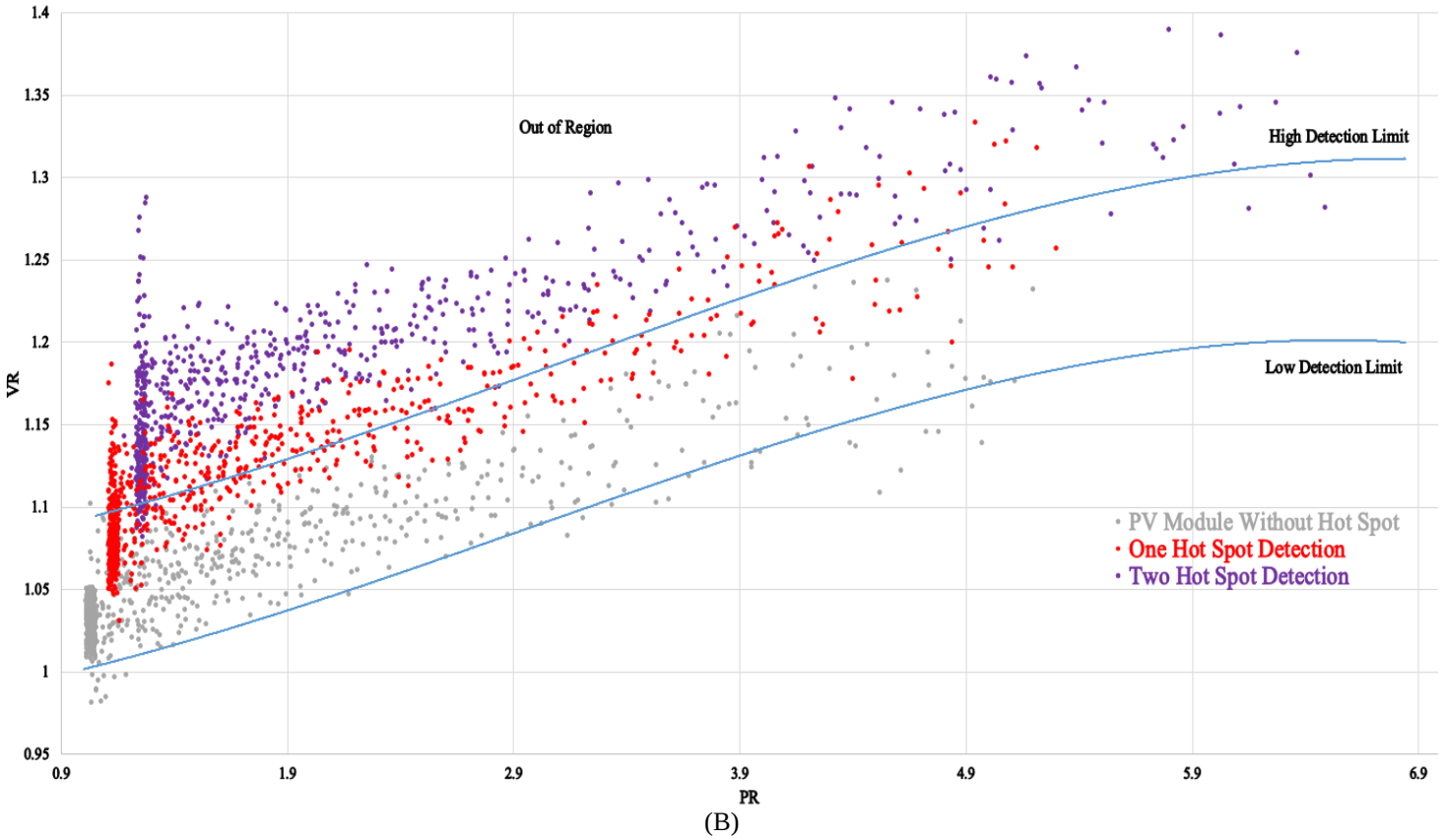

(B)

Fig. 14. Theoretical curves vs. real time long term measured data. (A) Hot spot images taken from two different PV modules using FLIR thermal imaging camera, (B) Theoretical fault detection curves vs. measured data obtained from a PV module without hot spots, PV module contains only one hot spot and PV module contains two hot spots

521 ***List of Tables:***

TABLE 1
Electrical Characteristics of SMT6 (60) P PV Module

Solar Panel Electrical Characteristics	Value
Peak Power	220 W
Voltage at maximum power point (V_{mp})	28.7 V
Current at maximum power point (I_{mp})	7.67 A
Open Circuit Voltage (V_{OC})	36.74 V
Short Circuit Current (I_{sc})	8.24 A
Number of cells connected in series	60
Number of cells connected in parallel	1
Rs , Rsh	0.48 Ω , 258.7 Ω
dark saturation current (Io)	2.8×10^{-10} A
Ideal diode factor (A)	0.9117
Boltzmann's constant (K)	1.3806×10^{-23} J.K^{-1}

TABLE 2
Efficiency Comparison between Four Different Case Scenarios

Test Number	**Case Scenario**	**Without Fuzzy Classifier**		**Including Fuzzy Classifier**	
		Out of Region Samples	Detection Accuracy (DA %)	Out of Region Samples	Detection Accuracy (DA %)
Test 1 (described in section 3.2)	Partial shading effects the GCPV system	37	94.86	5	99.31
Test 2 (presented as A in Fig. 11)	Faulty PV module and partial shading	34	95.27	7	99.03
Test 3 (presented as B in Fig. 11)	Two faulty PV module and partial shading	38	94.72	8	98.80
Test 4 (presented as C in Fig. 11)	Three faulty PV module and partial shading	37	94.86	5	99.31
Test 5 (presented as D in Fig. 11)	Four faulty PV module and partial shading	43	94.03	6	99.16

TABLE 3
Comparative Results between the Proposed Algorithm and the One Presented in Ref. [4], Ref. [7] and Ref. [8]

Case Study		Proposed Algorithm	Ref. [4]	Ref. [7]	Ref. [8]
Year of the Study		2017	2016	2015	2010
Software Used in the Data Analysis		LabVIEW	Not mentioned	Not mentioned	Not mentioned
PV System Capacity		1.1 kWp	Analysis on Single PV modules	1st : 3 kWp 2nd : 900 Wp	3.2 kWp
Fault Detection Algorithm Approach	Used Variables	Using power and voltage ratios	Using I-V curve	Current and voltage ratios	Current, voltage and power ratios
	Mathematical Modelling	3rd order polynomial function	Not used	Not used	Not used
	Statically Analysis Technique	Using T-test method	Not used	Not used	± 2 Standard Deviation
	Machine Learning Technique	Using Fuzzy logic system	Not used	Not used	Not used
Type of the Fault Detected	Partial Shading Conditions	√	√	√	√
	Faulty PV Modules	√	×	√	√
	Hot Spots	√	√	×	×